FEBS Letters 514 (2002) 204–208 FEBS 25839

Functional distinction of human EAG1 and EAG2 potassium channels

Roland Schönherr, Guido Gessner, Karsten Löber, Stefan H. Heinemann*

Arbeitsgruppe Molekulare und Zelluläre Biophysik, am Klinikum der Friedrich-Schiller-Universität Jena, Drackendorfer Straße 1, D-07747 Jena, Germany

Received 7 January 2002; accepted 17 January 2002

First published online 12 February 2002

Edited by Maurice Montal

Abstract Human ether à go-go potassium channel 2 (hEAG2) was cloned and its properties were compared with the previously characterized isoform hEAG1. In the *Xenopus* oocyte expression system the time course of activation was about four times slower and the voltage required for half-maximal subunit activation was about 10 mV greater for hEAG2 channels. However, its voltage dependence was smaller and, therefore, hEAG2 channels start to open at more negative voltages than hEAG1. Coexpression of both isoforms and kinetic analysis of the resulting currents indicated that they can form heteromeric channel complexes in which the slow activation phenotype of hEAG2 is dominant. Upon expression in mammalian cells, quinidine blocked hEAG1 channels (IC_{50} 1.4 μM) more potently than hEAG2 channels (IC_{50} 152 μM), thus providing a useful tool for the functional distinction between hEAG1 and hEAG2 potassium channels. © 2002 Published by Elsevier Science B.V. on behalf of the Federation of European Biochemical Societies.

Key words: Potassium channel; Ether à go-go; Coassembly; Quinidine

1. Introduction

Mutations in the ether à go-go gene (*eag*) in *Drosophila melanogaster* increase neuronal excitability and cause repetitive firing of motoneurons [1]. Heterologous expression of *eag* in *Xenopus* oocytes revealed typical properties of an outwardly rectifying, voltage-activated potassium channel [2]. Mammalian EAG channels have been cloned from rat, mouse, bovine and human and were characterized in heterologous expression systems [3–6].

As a common feature of EAG channels, hyperpolarizing prepulses slow down activation. This effect becomes most prominent in the presence of extracellular Mg^{2+} [3,7]. A second, distinctive phenotype is the current inhibition by Ca^{2+}/calmodulin, binding to the C-terminal domain [8,9].

EAG currents were identified in various cancer cell lines [10–12], leading to the hypothesis that EAG may have a role in malignant transformation. Pardo and coworkers [13] found that stable transfection of Chinese hamster ovary (CHO) cells with rEAG increased the proliferation rate and enhanced tumor formation in a mouse model. It was proposed that reduction of the membrane resting potential, caused by EAG, promotes cell cycle progression. Such hyperpolarizing activity of EAG channels was recently described for differentiating human myoblasts. Human (h) EAG channels are transiently expressed in these cells and hyperpolarize the membrane to induce myoblast fusion [6,14].

EAG channels are strongly expressed in brain [3,6]. The physiological function in the central nervous system, however, remains to be elucidated. The recent cloning of a second isoform of EAG from rat (rEAG2) and its restricted expression in brain and testes has drawn further attention on the role of both isoforms in the central nervous system [15,16]. Unfortunately, functional analysis of the channels in neuronal cells is hampered by the lack of potent blockers. Both EAG1 and EAG2 were found to be quite insensitive to typical potassium channel blockers [3,15]. In addition, the identification of functional differences will be required to discriminate both isoforms and to address their specific functions. Although a direct quantitative comparison with rEAG1 in the same expression system is still lacking, it was concluded that rEAG2 channels have a lower threshold for activation [17].

Here we describe the cloning of the hEAG2 isoform and its functional expression in *Xenopus* oocytes. We directly compare gating properties as well as pharmacological characteristics of hEAG2 and hEAG1 channels and describe practical tools for the discrimination of both isoforms.

2. Materials and methods

2.1. Cloning of hEAG2 and construction of expression plasmids

hEAG2 (GenBank accession number AF418206) was cloned from a human brain cDNA phage library (Clontech, Heidelberg, Germany) using a PCR screening approach with primers based on a published EST sequence (accession number U69185). The full-length open reading frame was sequenced and inserted into the oocyte expression vector pGEM-HE [18] and the mammalian expression vector pcDNA3 (Invitrogen, Groningen, The Netherlands). Insertion of hEAG1 (accession number AJ001366) into the same vector was described previously [9]. mRNA was synthesized with the T7 mMESSAGE mMACHINE kit (Ambion, Austin, TX, USA). Two point mutants of hEAG1 (L322H and G440C) were generated in two-step PCR reactions.

2.2. Functional expression in Xenopus oocytes

Stage V oocytes were obtained from *Xenopus laevis* after ice–water/tricaine anesthesia. Cells were injected with 50 nl of mRNA (5–500 ng/μl). Currents were recorded at 20 ± 0.5°C 1–4 days after injection. Two-electrode voltage clamp was performed with a Turbo-TEC 10CD amplifier (NPI electronic, Tamm, Germany). The bath solution contained (in mM): 115 NaCl, 2.5 KCl, 1.8 $CaCl_2$, 10 HEPES, pH 7.2 (NaOH) plus the indicated concentration of $MgCl_2$. Tail currents were measured in 40K-Ringer solution (in mM): 75 NaCl, 40 KCl,

*Corresponding author. Fax: (49)-3641-304 542.
E-mail address: stefan.h.heinemann@uni-jena.de (S.H. Heinemann).

Abbreviations: TEA, tetraethylammonium; EAG, ether à go-go

0014-5793/02/$22.00
PII: S0014-5793(02)02365-7

1.8 $CaCl_2$, 10 HEPES, pH 7.2 (NaOH). Experiment control was performed with the Pulse+PulseFit software package (HEKA elektronik, Lambrecht, Germany). Leak and capacitance currents were corrected with a *P/n* method. Pooled data are represented as means ± S.E.M. (n = number of independent experiments).

Current activation was analyzed with a kinetic model described earlier [19]. It is assumed that each of the four individual subunits of the channel can reside in three states: slow, fast, and activated. Transitions between 'slow' and 'fast' occur slowly, characterized with the time constant τ_{slow}. The probability to find a subunit in 'slow' is P_{slow}. Transitions from 'fast' to 'activated' correspond to the rapid activation of voltage-gated potassium channels. In this model they are lumped by a single exponential activation phase with time constant τ_{fast}. For simplicity the model further assumes that channels only can undergo the fast transitions when all four subunits have performed the first step. Mathematically this can be expressed as sum of simple time courses distributed binomially:

$$I(t) = a\left\{(1-P_{slow})^4(1-e^{-1/\tau_{fast}})+ \left[\sum_{i=1}^{4}\binom{4}{i}P_{slow}^{i}(1-P_{slow})^{4-i}(1-e^{-t/\tau_{slow}})^{i}\right]\right\} \quad (1)$$

In the two-electrode voltage clamp the time resolution is not high enough to faithfully resolve τ_{fast}. Thus, analysis of current traces in response to voltage steps yields two relevant parameters: τ_{slow} and P_{slow}. The voltage dependence of P_{slow} was fit with Boltzmann functions:

$$P_{slow}(V) = \frac{P_{-\infty}}{1+e^{-(V-V_h)/k}} \quad (2)$$

with the half-maximal activation voltage V_h and a slope factor k that characterizes the voltage dependence.

Channel activation, i.e. channel open probability P_o, was described with fourth order Boltzmann functions fitted to tail current data:

$$P_0(V) = \frac{1}{(1+e^{-(V-V_h)/k})^4} \quad (3)$$

2.3. Functional expression in mammalian cell lines

CHO cells were transfected using the superfect reagent (Qiagen, Hilden, Germany). Borosilicate glass patch pipettes were filled with (in mM): 130 KCl, 2 $MgCl_2$, 10 EGTA, 10 HEPES, pH 7.4 (KOH). The bath solution contained (in mM): 145 NaCl, 5 KCl, 2 $MgCl_2$, 2 $CaCl_2$, 10 HEPES, pH 7.4 (NaOH). Currents were measured with an EPC9 patch clamp (HEKA elektronik) in the whole-cell configuration with access resistances below 5 MΩ. Series resistance was compensated for 70–85%.

Effects of channel blockers were allowed to equilibrate by repetitive pulsing phases of at least 5 min. Current block was analyzed by measuring the current at the end of a 1-s depolarization to +50 mV. The

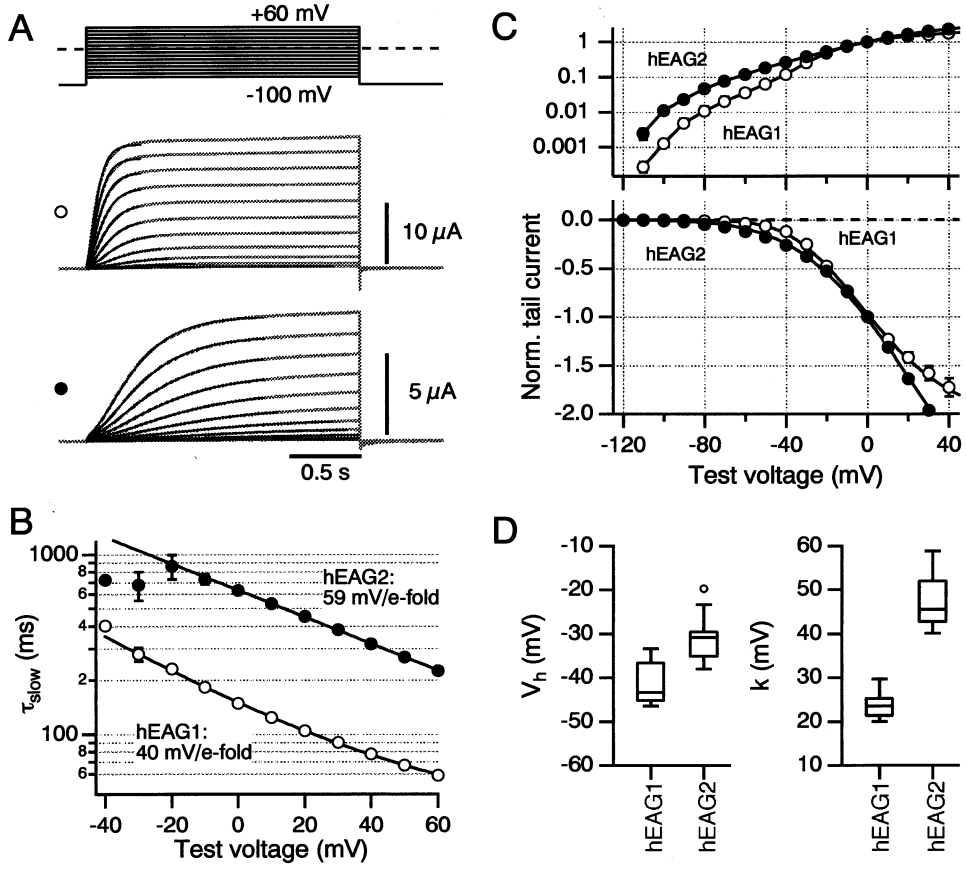

Fig. 1. Current–voltage relationships of hEAG1 and hEAG2 channels expressed in *Xenopus* oocytes. A: Activation time courses of hEAG1 (○) and hEAG2 (●) in response to 2-s depolarizing pulses from a holding potential of −100 mV. The extracellular solution contained 5 mM Mg^{2+}. The superimposed curves indicate data fits according to Eq. 1. B: τ_{slow} from fits in A as a function of the test voltage (n = 6). Under these conditions P_{slow} was 0.57 for both hEAG1 and hEAG2. The curves are single exponential fits to estimate the voltage dependence: 40 mV/e-fold for hEAG1 and 59 mV/e-fold for hEAG2. C: In 40K-Ringer solution 2-s depolarizations were applied and peak inward tail current amplitudes were measured at −100 mV. These were normalized to the value at 0 mV and plotted versus the test voltage on a semi-logarithmic (upper panel) and linear scale (below) (n = 6). In the upper panel symbols are connected by straight lines. The continuous curves in the linear plot are fits to Eq. 3 yielding V_h and k that are shown in D as box plots.

concentration dependence of block was described with a Hill equation:

$$\frac{I}{I_{\text{contr}}}(c) = \frac{\left(\frac{\text{IC}_{50}}{c}\right)^{h}}{1+\left(\frac{\text{IC}_{50}}{c}\right)^{h}} \quad (4)$$

with the Hill coefficient h.

3. Results and discussion

3.1. Voltage dependence and kinetics of channel activation

The hEAG2 potassium channel was cloned from a cDNA library. The derived amino acid sequence displays 73% identity with hEAG1, exhibiting the highest divergence between the cytoplasmic C-termini [6]. 98% identical residues are shared between hEAG2 and the orthologue protein from rat, rEAG2 [15]. For direct comparison of the hEAG isoforms, we expressed both channels in *Xenopus* oocytes and measured currents with a two-electrode voltage clamp. Despite identical expression vector constructs, mRNA for hEAG2 consistently yielded lower current amplitudes compared to hEAG1. Equal current levels were obtained by about 20-fold higher dilution of hEAG1 mRNA. Channel activation was assayed by depolarizing voltage steps (Fig. 1A). In the presence of 5 mM Mg^{2+}, both channel types generated slowly activating currents without inactivation. The kinetics of channel activation were analyzed by fitting the EAG activation model (Eq. 1) to the data (see methods). The resulting values for τ_{slow} are plotted in Fig. 1B as a function of the test voltage. It is clearly seen that hEAG2 channels activate more slowly, at +40 mV by a factor of about 4. The voltage dependence of the activation time constants was weaker for hEAG2 than for hEAG1 (Fig. 1B).

Inward tail current amplitudes were measured in Mg^{2+}-free 40K-Ringer to assay steady-state activation (Fig. 1C). hEAG2 channels activate at lower voltages than hEAG1 channels. At −80 mV hEAG2 current already reached 4.5% of the current at 0 mV, compared to 1.1% for hEAG1. The current–voltage relationships were fitted according to Eq. 3 and the resulting V_{h} and k values are shown in Fig. 1D. The half-activation voltage of hEAG2 subunits (−30.9 mV) was greater than for hEAG1 subunits (V_{h} −43.3 mV). However, the slope factor k for hEAG2 (median 45.6 mV) was consistently greater than that for hEAG1 (median 23.6 mV), resulting in a lower activation threshold for hEAG2 channels.

In accordance with the early activation of both channel types, we consistently observed resting potentials below −70 mV in 2.5 mM extracellular K^+ solution when oocytes expressed either of the hEAG isoforms. In comparison, oocytes expressing hKv1.5 potassium channels with similar current amplitudes (10–20 μA at +40 mV) had resting potentials of about −40 mV. The stronger hyperpolarizing activity of EAG channels in oocytes suggests an impact on neuronal resting potentials and excitability.

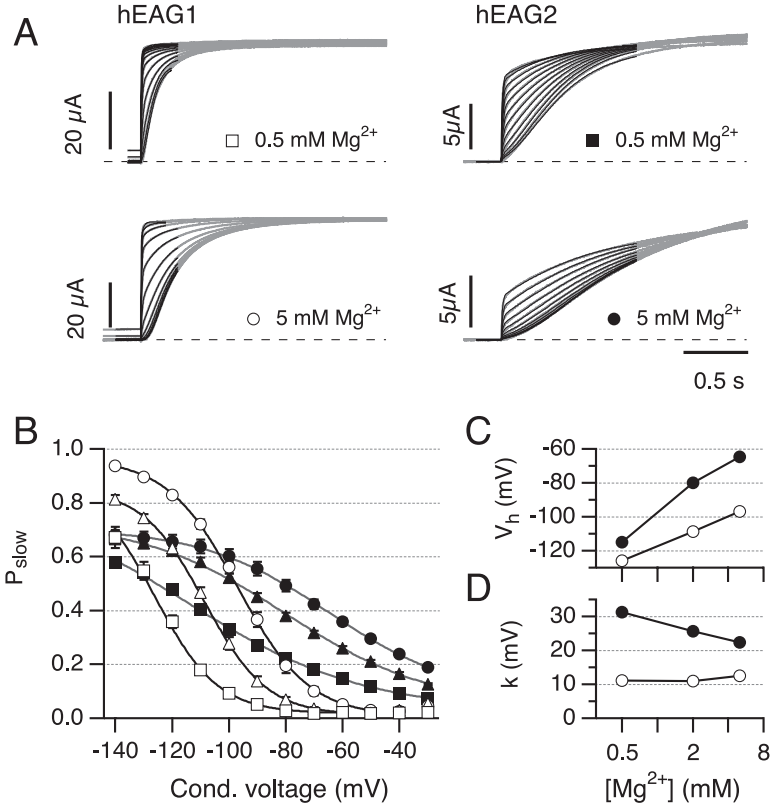

Fig. 2. Prepulse dependence of hEAG activation. A: Current traces of hEAG1 and hEAG2 channels, expressed in *Xenopus* oocytes with the indicated concentrations of Mg^{2+} in the bath solution. The pulse protocol was a depolarization to +40 mV preceded by 5-s intervals at prepulse voltages ranging from −140 to −30 mV. The superimposed curves (black) are results of data fits according to Eq. 1. B: P_{slow} derived from data fits as shown in A for hEAG1 (open symbols) and hEAG2 (filled symbols) ($n = 3$) for 0.5 (squares), 2.0 (triangles), and 5.0 mM Mg^{2+} (circles). The curves are fit results according to first- order Boltzmann functions Eq. 2. The resulting half-maximal voltage, V_{h}, and slope factor, k, are plotted in C and D as a function of the Mg^{2+} concentration.

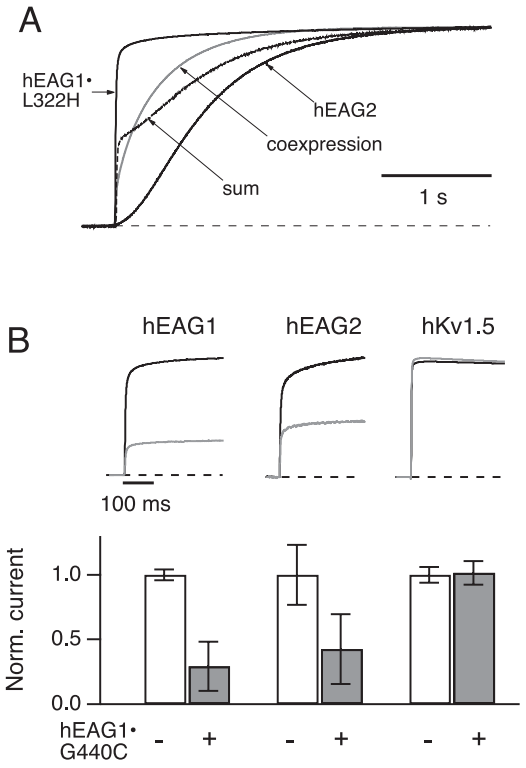

Fig. 3. Coassembly of hEAG1 and hEAG2 subunits. A: The rapidly activating mutant hEAG1·L322H, wild-type hEAG2 channels and a mixture of both were expressed in oocytes. Test pulses to +40 mV were elicited after 5-s hyperpolarization to −130 mV in bath solution with 5 mM Mg^{2+}. Average currents from six oocytes of each group were normalized and superimposed. Currents from coinjected cells show intermediate kinetics, which cannot be described as a sum of fast and slow traces (dotted line). B: mRNA for hEAG1, hEAG2 and hKv1.5 channels was injected into *Xenopus* oocytes in concentrations leading to equal current amplitudes. In parallel injections the same mRNAs were coinjected with a dominant negative mutant of hEAG1 (G440C). Averaged current traces from 40-mV test pulses are shown for the absence (black) and presence (gray) of the mutant. The bar graphs show the normalized amplitudes in comparison to mean amplitudes of coinjections. $n = 13$–15.

3.2. Prepulse dependence of channel activation

A typical feature of EAG channels is the dependence of activation kinetics on the holding potential and the concentration of extracellular Mg^{2+} [7]. We measured channel activation in 0.5, 2, and 5 mM Mg^{2+} under variation of the prepulse voltage. Fig. 2A shows current traces for experiments with hEAG1 and hEAG2 with superimposed fits according to Eq. 1. The values for P_{slow} as a function of the conditioning voltage are shown in Fig. 2B, clearly indicating that hEAG2 channels do reach a smaller limiting P_{slow} at very negative voltages. However, the voltage dependence of P_{slow} in hEAG2 is smaller, leading to a cross-over of the curves. Thus, at neuronal resting potentials, i.e. around −80 mV, the probability for slow activation of hEAG2 subunits is higher than for hEAG1 subunits. The observation was quantified by Boltzmann fits yielding half-maximal voltages and slope factors shown in Fig. 2C,D. At physiological Mg^{2+} concentrations (2 mM) the half-maximal voltage for slow activation of hEAG2 channels is −80 mV compared to −107 mV for hEAG1 channels.

This analysis revealed functional differences between both channels: the main characteristics of hEAG2 are a slower activation time course and a smaller voltage dependence, which is seen for steady-state activation (Fig. 1D) as well as in the P_{slow}–V relation (Fig. 2B). The molecular background for this difference is not yet clear, as all residues in the voltage sensor domains (S4) of both isoforms are conserved.

3.3. Coassembly of hEAG1 and hEAG2 subunits

Both isoforms of rEAG channels share some regions of similarly high expression, e.g. cerebral cortex, amygdala and olfactory bulb [16,17]. Thus, it is important to know whether they can form heteromeric channels with intermediate phenotypes. We coinjected mRNA for hEAG1 and hEAG2 at various ratios and analyzed the activation kinetics and the voltage dependence of P_{slow}. The resulting currents were compatible with a mixing of hEAG1 and hEAG2 subunits (not shown), but homomeric channels could not safely be excluded. For an unambiguous analysis we enhanced the kinetic differences between the subunits, using a point mutation in the S3–S4 linker region of hEAG1 (L322H) leading to faster activation [19]. Current traces for individual channels and coinjections of hEAG1·L322H and hEAG2 are shown in Fig. 3A. Mutant hEAG1 channels showed fast activation in the presence of 5 mM Mg^{2+}, while hEAG2 currents had the typical sigmoidal rising phase. Currents in coinjected oocytes could not be explained as the sum of both individual time courses (dotted line), suggesting heteromeric channel formation. Further evidence for heteromeric assembly came from a dominant negative mutant of hEAG1 (mutation G440C in the selectivity filter) that did not yield current in *Xenopus* oocytes. However, coexpression of hEAG1·G440C with either hEAG1

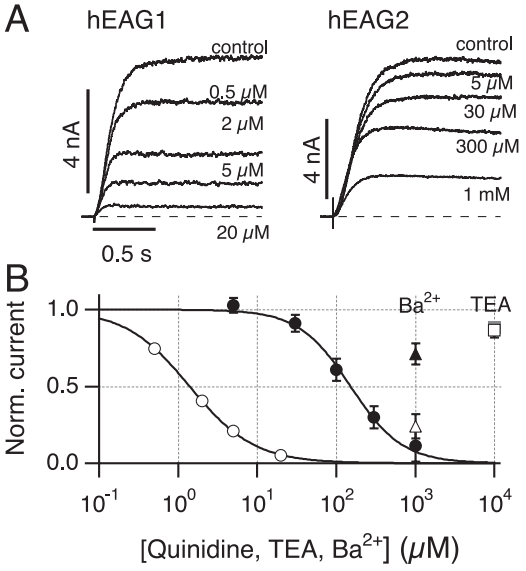

Fig. 4. Block of hEAG channels in mammalian cells. A: Current traces in response to depolarizations to +50 mV from a holding voltage of −100 mV from hEAG1 (left) and hEAG2 (right) channels expressed in CHO cells under control conditions and after application of the indicated concentrations of quinidine. B: Dose–response plots of hEAG1 (open circles) and hEAG2 (filled circles) for quinidine ($n = 4$–6). The curves indicate fits according to Eq. 4. Also included are responses to 10 mM TEA (squares, $n = 4$ or 5) and 1 mM $BaCl_2$ (triangles, $n = 5$) for hEAG1 (open symbols) and hEAG2 (filled symbols).

or hEAG2 resulted in a reduction of current (Fig. 3B). Coexpression with the non-related hKv1.5 channel did not significantly reduce the current.

We conclude that both hEAG isoforms interact and form heteromeric channels. EAG heteromultimer formation could thereby increase the functional variability of EAG currents in regions of overlapping expression. The same was proposed for the related ERG channels, which formed heteromers in vitro, but did not interact with rEAG1 [20].

3.4. Pharmacological differences between hEAG1 and hEAG2 channels

EAG channels have been described as channels with low sensitivity to classical channel blockers like tetraethylammonium (TEA) or 4-amino-pyridine or the HERG blocker E4031 [15,21]. We chose mammalian cells for a pharmacological characterization, to allow direct comparison to native currents. TEA, applied at 10 mM, only blocked the channels by about 10% at +50 mV without significant difference between hEAG1 and hEAG2 ($P = 0.76$, two-sided t-test). Ba^{2+} ions extracellularly applied at a concentration of 1 mM inhibited hEAG1 channels to $24 \pm 8\%$ of the control current, while hEAG2 currents were only reduced to $71 \pm 7\%$ ($n = 5$, $P = 0.025$). Quinidine, however, blocked hEAG1 with an IC_{50} value of 1.4 ± 0.06 μM. In contrast, hEAG2 channels were about 100-fold less sensitive (IC_{50} 151.8 ± 24.8 μM) (Fig. 4). Thus, quinidine can be used as a blocker of hEAG1 channels in mammalian cells. In oocytes, a much lower sensitivity has been reported for rEAG1 (IC_{50} 400 μM), underlining the value of mammalian expression systems for pharmacological studies [3].

In summary, the slower activation, the lower voltage dependence and significantly lower quinidine sensitivity of hEAG2 channels provide tools to discriminate both isoforms of EAG channels in neurons and cancer cells.

Acknowledgements: We are grateful for assistance by S. Arend and A. Roßner. This work was supported by the Max Planck Society and the DFG (He 2993/2, 2993/4).

References

[1] Ganetzky, B. and Wu, C.F. (1983) J. Neurogenet. 1, 17–28.
[2] Brüggemann, A., Pardo, L.A., Stühmer, W. and Pongs, O. (1993) Nature 365, 445–448.
[3] Ludwig, J., Terlau, H., Wunder, F., Brüggemann, A., Pardo, L.A., Marquardt, A., Stühmer, W. and Pongs, O. (1994) EMBO J. 13, 4451–4458.
[4] Robertson, G.A., Warmke, J.W. and Ganetzky, B. (1996) Neuropharmacology 35, 841–850.
[5] Frings, S., Brüll, N., Dzeja, C., Angele, A., Hagen, V. and Kaupp, U.B. (1998) J. Gen. Physiol. 111, 583–599.
[6] Occhiodoro, T., Bernheim, L., Liu, J.-H., Bijlenga, P., Sinnreich, M., Bader, C.R. and Fischer-Lougheed, J. (1998) FEBS Lett. 434, 177–182.
[7] Terlau, H., Ludwig, J., Steffan, T., Pongs, O., Stühmer, W. and Heinemann, S.H. (1996) Pflüg. Arch. 432, 301–312.
[8] Stansfeld, C.E., Röper, J., Ludwig, J., Weseloh, R.M., Marsh, S.J., Brown, D.A. and Pongs, O. (1996) Proc. Natl. Acad. Sci. USA 93, 9910–9914.
[9] Schönherr, R., Löber, K. and Heinemann, S.H. (2000) EMBO J. 19, 3263–3271.
[10] Meyer, R. and Heinemann, S.H. (1998) J. Physiol. 508, 49–56.
[11] Meyer, R., Schönherr, R., Gavrilova-Ruch, O., Wohlrab, W. and Heinemann, S.H. (1999) J. Membr. Biol. 171, 107–115.
[12] Ouadid-Ahidouch, H., Le-Bourhis, X., Roudbaraki, M., Toillon, R.A., Delcourt, P. and Prevarskaya, N. (2001) Recept. channels 1, 61–71.
[13] Pardo, L.A., del Camino, D., Sánchez, A., Alves, F., Brüggemann, A., Beckh, S. and Stühmer, W. (1999) EMBO J. 18, 5540–5547.
[14] Bijlenga, P., Occhiodoro, T., Liu, J.H., Bernheim, L. and Fischer-Lougheed, J. (1998) J. Physiol. 512, 317–323.
[15] Saganich, M.J., Vega-Saenz de Miera, E., Nadel, M.S., Baker, H., Coetzee, W.A. and Rudy, B. (1999) J. Neurosci. 19, 10789–10802.
[16] Ludwig, J., Weseloh, R., Karschin, C., Liu, Q., Netzer, R., Engeland, B., Stansfeld, C. and Pongs, O. (2000) Mol. Cell. Neurosci. 16, 59–70.
[17] Saganich, M.J., Machado, E. and Rudy, B. (2001) J. Neurosci. 21, 4609–4624.
[18] Liman, E.R., Tytgat, J. and Hess, P. (1992) Neuron 9, 861–871.
[19] Schönherr, R., Hehl, S., Terlau, H., Baumann, A. and Heinemann, S.H. (1999) J. Biol. Chem. 274, 5362–5369.
[20] Wimmers, S., Wulfsen, I., Bauer, C.K. and Schwarz, J.R. (2001) Pflüg. Arch. 441, 450–455.
[21] Engeland, B., Neu, A., Ludwig, J., Roeper, J. and Pongs, O. (1998) J. Physiol. 513, 647–654.